Separation of arsenic and antimony from dust with high content of arsenic by a selective sulfidation roasting process using sulfur

Cheng TAN, Lei LI, Da-peng ZHONG, Hua WANG, Kong-zhai LI

State Key Laboratory of Complex Non-ferrous Metal Resources Clean Utilization,
Engineering Research Center of Metallurgical Energy Conservation and Emission Reduction of Ministry of Education,
Faculty of Metallurgical and Energy Engineering,
Kunming University of Science and Technology, Kunming 650093, China

Abstract: The separation of arsenic and antimony from dust with high content of arsenic was conducted via a selective sulfidation roasting process. The factors such as roasting temperature, roasting time, sulfur content and nitrogen flow rate were investigated using XRD, EPMA and SEM−EDS. In a certain range, the sulfur addition has an active effect on the arsenic volatilization because the solid solution phase (($Sb,As)_2O_3$) in the dust can be destroyed after the Sb component in it being vulcanized to Sb_2S_3 and this generated As_2O_3 continues to volatile. In addition, an amorphization reaction between As_2O_3 and Sb_2O_3 is hindered through the sulfidation of Sb_2O_3, which is also beneficial to increasing arsenic volatilization rate. The results show that volatilization rates of arsenic and antimony reach 95.36% and only 9.07%, respectively, under the optimum condition of roasting temperature of 350 °C, roasting time of 90 min, sulfur content of 22% and N_2 flow rate of 70 mL/min. In addition, the antimony in the residues can be reclaimed through a reverberatory process.

Key words: dust; arsenic; antimony; sulfur; selective sulfidation roasting; separation

1 Introduction

Arsenic is a toxic and carcinogenic element that has aroused major public concern [1], and the arsenic pollution has become a global problem, reported frequently in many countries such as America, Japan, India, Mexico and China. The pilling-up of substances containing arsenic will release poison into the groundwater [2,3]. Besides, the world reserve amount of antimony is higher than two million tones, most of which is found in China, Bolivia, Russia and South Africa [4]. Among them, China has the largest antimony resource, but the uncontrolled exploitation causes the antimony ore to be exhausted in ten years. It is therefore necessary to find other resources from which antimony can be extracted besides its ore.

Massive dust with high content of arsenic and antimony is generated from nonferrous pyrometallurgical industries. The dust not only represents potential hazard to the environment but also is a secondary resource [5], which should be properly treated and utilized to obtain the maximum economic and environmental benefits [6−8]. The dust can not be directly recycled to the antimony smelting process, due to high arsenic content. It is necessary to treat the dust individually to remove arsenic and recover the antimony resource.

Based on distinctions of volatility [9] and water-solubility [10] of arsenic and antimony compounds, the treatment of dust with high content of arsenic and antimony can be classified into two methods: pyrometallurgical and hydrometallurgical processes. The pyrometallurgical process generally involves oxidizing roasting and reduction roasting, in which the arsenic is volatilized in the form of As_4O_6 and thereafter collected and the antimony retains in the form of Sb_2O_3 or Sb_2O_4, but the separation rate is low [11,12]. To overcome this disadvantage, variety of hydrometallurgical processes for removing arsenic using sodium−sulfide solution [13], oxygen pressure leaching in NaOH solution [14] etc have

been developed. Although these hydrometallurgical methods are considered to be high efficient for the separation of arsenic, they consume a great deal of chemical reagents and possess complicated technological process.

In this work, a novel method for treating dust with high content of arsenic and antimony via a selective sulfidation roasting process is proposed. The sulfur was used as a sulfidation agent participating in the roasting. The influence of processing parameters had been investigated systematically in order to determine the optimal conditions for increasing the separation rate of arsenic and antimony, including roasting temperature, addition amount of sulfur, roasting time and N_2 flow rate.

2 Experimental

2.1 Materials and analysis

The dust with high content of arsenic and antimony used in this work was provided by a plant which treated tin anode slime through a pyrometallurgical process, located in Yunnan province, China. Nitrogen (purity of 99.3%) was procured from local suppliers. Sulfur (>99.5%, synthetic powder) was used as the sulfidation agent. Phase compositions of the dust and sulfur were detected by an X-ray diffraction using a diffractometer (TTRIII, Japan) under the conditions as follows: Cu K_α, tube current and voltage: 200 mA and 40 kV, scanning range: 10°−90° (2θ), step size: 0.02° (2θ) and scanning speed: 10 (°)/min. Figure 1 shows that the phase of sulfur used is S_8. Figure 2 indicates that arsenolite (As_2O_3, cubic), As_4O_6, senarmontite (Sb_2O_3, cubic), and solid solution (($Sb,As)_2O_3$) [11] are major phases in the dust. The mineral constituent of the dust was analyzed using EPMA instrument (EMPA−1600). Figure 3 shows that some arsenic and antimony exist independently in the form of arsenolite and senarmontite, respectively. Meanwhile, some mineral phases containing both As and Sb are also observed, including variant white arsenic ore,
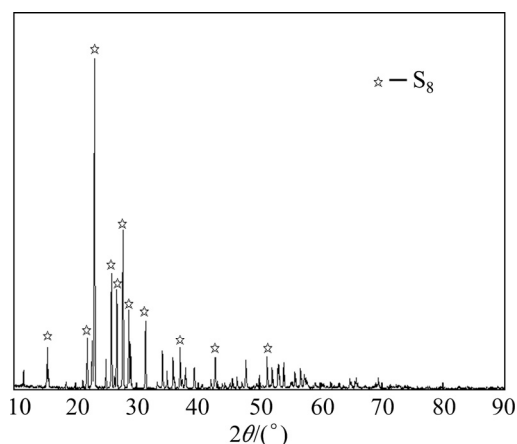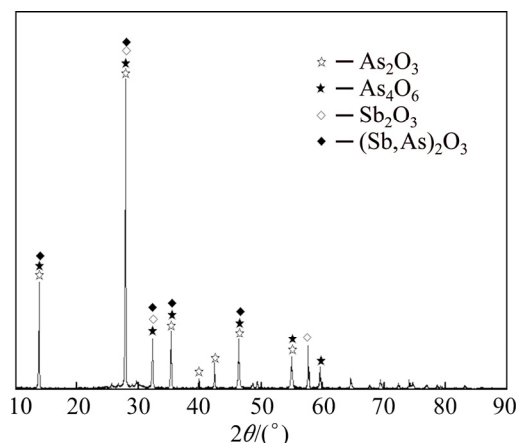

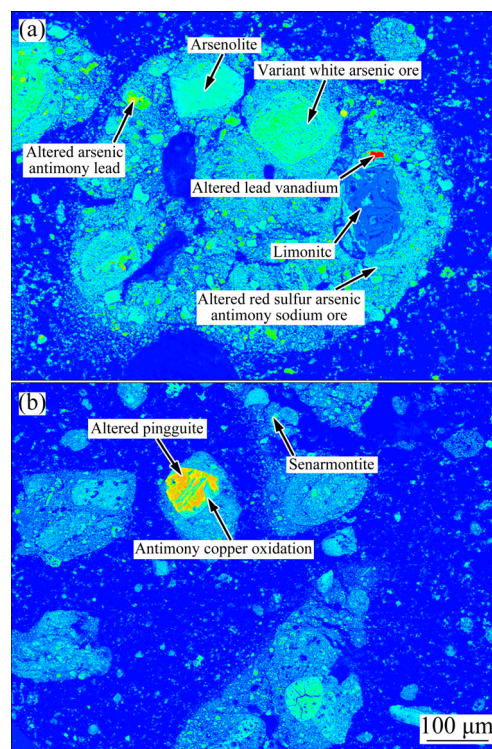**Fig. 2** X-ray diffraction pattern of raw material

Fig. 3 Raw mineral constituents obtained by EPMA

altered arsenic antimony lead ore and altered red sulfur arsenic antimony sodium ore. Chemical compositions of the dust and the roasted residues were characterized by chemical analysis. Especially, XRF analysis (MINIPAL4, PANalytical, Netherlands) was used to detect the O content in the dust. The primary chemical composition of the dust is given in Table 1. It is characterized by high arsenic (36.28%) and antimony (28.72%) contents, and the antimony is well worth reclaiming.

Fig. 1 X-ray diffraction pattern of sulfur

Table 1 Primary chemical composition of dust (mass fraction, %)

As	Sb	O	Se	Pb	Fe	Bi	Cu
36.28	28.72	22.35	2.46	2.06	1.13	0.68	0.24

2.2 Experimental procedure

The roasting experiments were conducted in an electric tube furnace (GSL−1500X, Hefei Kejing Materials Technology Co. Ltd., China), which is shown in Fig. 4. 5 g of the dust sample was used in every experiment, and addition amount of sulfur was calculated based on the mass ratio of the sulfur to the dust. Nitrogen was pumped into the tube furnace to expel the air before the furnace being preheated to the required temperature and then introduced continuously with a constant flow rate. A corundum crucible loading pulverized samples (particle size <74 μm) was introduced into the roasting zone when the temperature reached a required level. The sample was roasted at a set temperature for a certain time. Once roasting was completed, the crucible was cooled down in N_2 atmosphere. The off-gas from the reaction tube was continuously passed through an ice water bath, which collected the volatile matter, and then was directed to solutions of 1 mol/L NaOH to remove harmful components. Nonisothermal experiments were conducted using a thermal analyzer (METTLER HT/1600) in the temperature range of 25−500 °C with heating rate of 5 °C/min in nitrogen atmosphere. The volatilization rates α and β for As and Sb were calculated using the following formulas:

$$\alpha = (1 - \frac{m \times w_A}{m_0 \times w_{A0}}) \times 100\% \tag{1}$$

$$\beta = (1 - \frac{m \times w_S}{m_0 \times w_{S0}}) \times 100\% \tag{2}$$
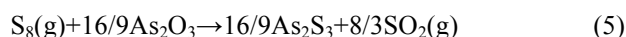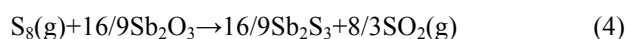
where m_0 and m stand for total masses of the initial samples and roasted residues, w_{A0} and w_{S0} are the contents of As and Sb (mass fraction, %) in the initial samples, and w_A and w_S are the contents of As and Sb (mass fraction, %) in the roasted residues, respectively.

3 Result and discussion

3.1 Thermodynamic analysis

In this work, thermodynamic calculations were performed to predict possible reactions during the roasting process. The standard Gibbs free energy changes of Eq. (3) for the transition from As_2O_3 to As_4O_6 (g) are negative when the temperature is above 350 °C and the value decreases continuously with the increase of temperature (Fig. 5). The Sb_2O_3 is more easily to be vulcanized due to more negative values of standard Gibbs free energy of Eq. (4) than Eq. (5) (Fig. 5).

$$As_2O_3 \rightarrow 1/2As_4O_6(g) \tag{3}$$

$$S_8(g) + 16/9Sb_2O_3 \rightarrow 16/9Sb_2S_3 + 8/3SO_2(g) \tag{4}$$

$$S_8(g) + 16/9As_2O_3 \rightarrow 16/9As_2S_3 + 8/3SO_2(g) \tag{5}$$

The Factsage 7.0 was used to calculate the equilibrium of roasted products in Gibbs free energy minimization under isothermal, isobaric and fixed mass conditions. Required data for computation was taken from FactPS and FToxid database of the programme. The calculations were performed for 1 mol Sb_2O_3 and 2 mol As_2O_3 for closing to the composition of the dust at variable amounts of sulfur in temperature range of 300−450 °C and atmosphere pressure of 1.01325×10^5 Pa. The phases of As_4O_6, As_2S_3, As_2O_3, Sb_2S_3, Sb_2O_3 and solid solutions containing As_3SbO_6, $As_2Sb_2O_6$ and $AsSb_3O_6$ are assumed to be present in roasted products and the results of equilibrium of phases are present in Fig. 6. Figure 6 shows that with sulfur amount being less than 0.5 (300 and 350 °C) or 0.45 (400 and 450 °C), there is no As_2S_3 existing in the roasted products and the main arsenic-containing phase is As_4O_6. Increasing the sulfur amount further, the amount of As_4O_6 decreases while that of As_2S_3 rapidly increases, which is due to the sulfidation of As_2O_3 by the sulfur. On the contrary, the amount of Sb_2S_3 always increases with sulfur amount. This could also indicate that Sb has a higher affinity for sulfur than As. In addition, the solid solution amount increases with temperature at the same sulfur amount, seen from Fig. 6, which goes against the separation of arsenic and antimony.

Figure 7 shows TG−DSC curves of the dust and mixed sample (the dust and sulfur, and sulfur content of 22%). Figure 7(a) is for the dust and Fig. 7(b) for the mixture. The endothermic peak centering at 275.67 °C in
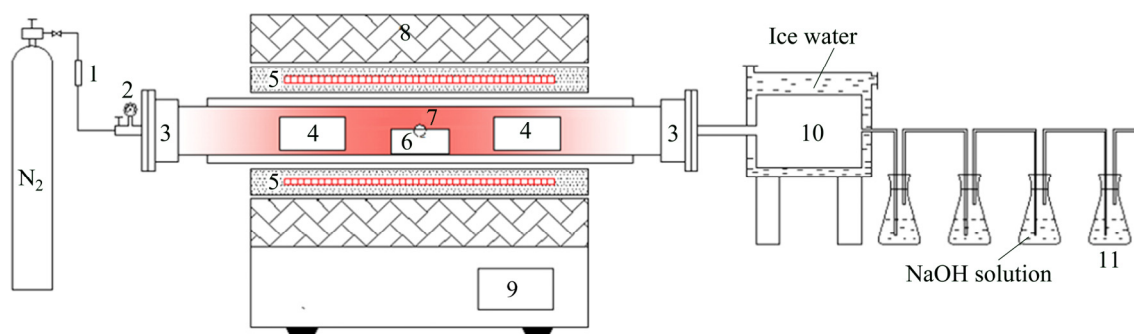

Fig. 4 Experimental apparatus: 1—Flowmeter; 2—Pressure gauge; 3—Flange; 4—Oven tap; 5—SiC heating component; 6—Sample boat; 7—Pt−Rh thermocouple; 8—Tube furnace; 9—Intelligent temperature controller; 10—Ice-water bath; 11—Conical flask
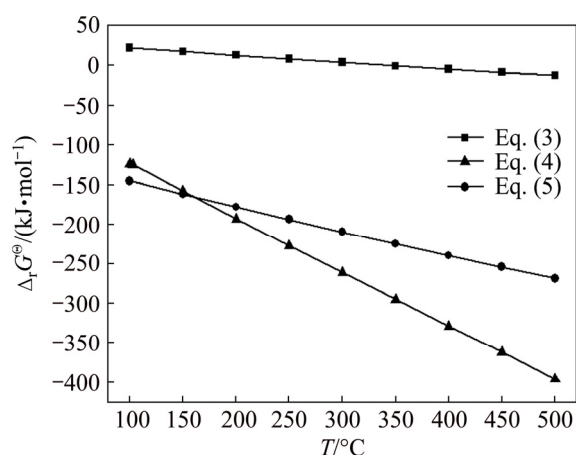
Fig. 5 Standard Gibbs free energy changes of reactions (3)−(5) in temperature range of 100−500 °C

Fig. 7(a) is caused by melting of As_2O_3 and vast volatilization of the dust. On the other hand, three noticeable endothermic peaks are detected in the DSC measurement for the mixture. The first peak at 106.08 °C is attributed to melting of the sulfur, and the second peak at 259.42 °C and third peak at 284.33 °C to volatilization of the sample. A larger mass-loss of 46.68% in Fig. 7(b)

compared with that of 22.72% in Fig. 7(a) occurs in the temperature range of 200−300 °C, which indicates that the sulfur can promote the dust volatilization effectively.

As mentioned above, the selective sulfidation roasting of the dust with high content of arsenic and antimony should be performed with a small sulfur amount at a low temperature to obtain a maximum separation rate between arsenic and antimony.

3.2 Effect of roasting temperature

In order to investigate the effect of roasting temperature on the separation of arsenic and antimony, experiments were performed at 250−450 °C while keeping other parameters constant as sulfur content of 22%, roasting time of 90 min and N_2 flow rate of 70 mL/min. In addition, a blank test without sulfur was also carried out under the same condition.

BROOKS et al [15] reported that As_2O_3 could be reacted with Sb_2O_3 and formed an amorphous substance (As−Sb−O) at a temperature higher than 300 °C, which inhibits the arsenic volatilization and simultaneously promotes the antimony volatilization. This amorphous substance exhibits vapor pressure difference from that of its individual parent compounds, which is lower than
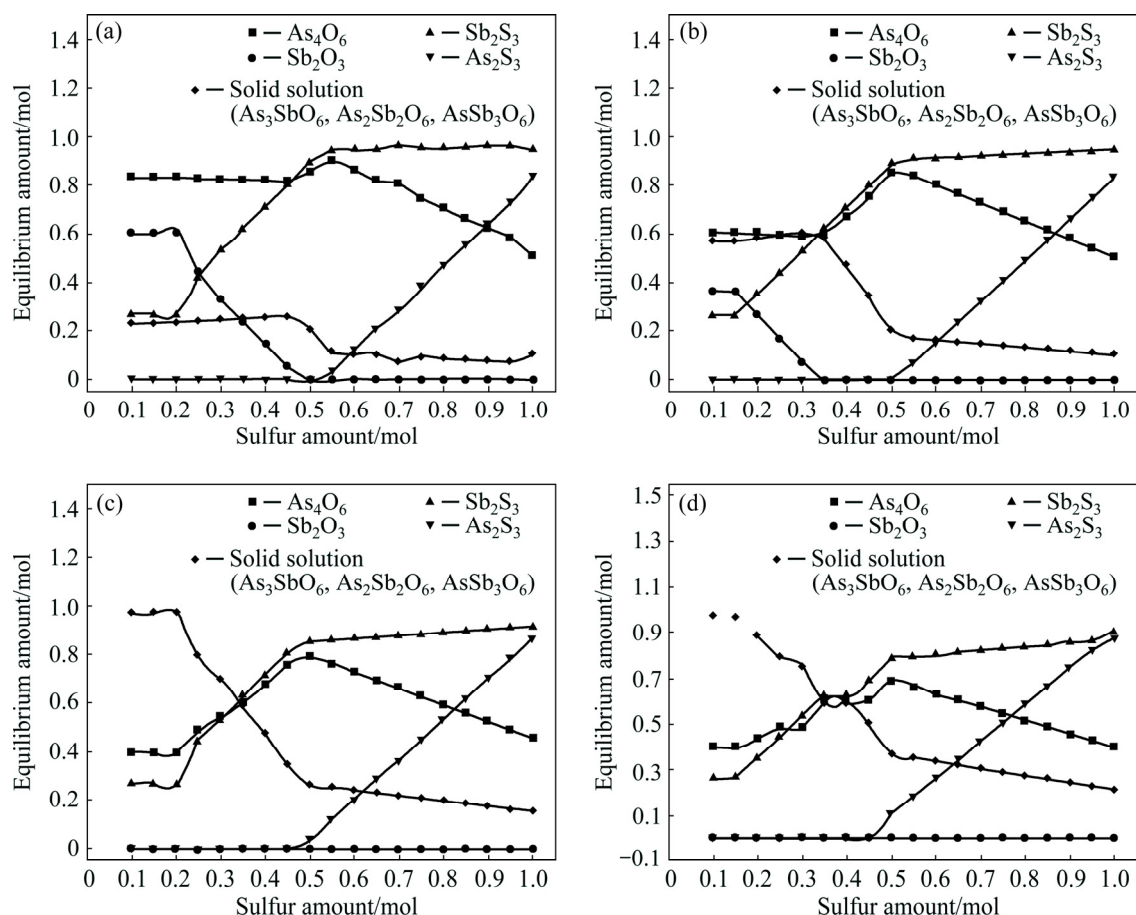

Fig. 6 Equilibrium amounts of arsenic and antimony in roasted products as function of sulfur amount: (a) 300 °C; (b) 350 °C; (c) 400 °C; (d) 450 °C
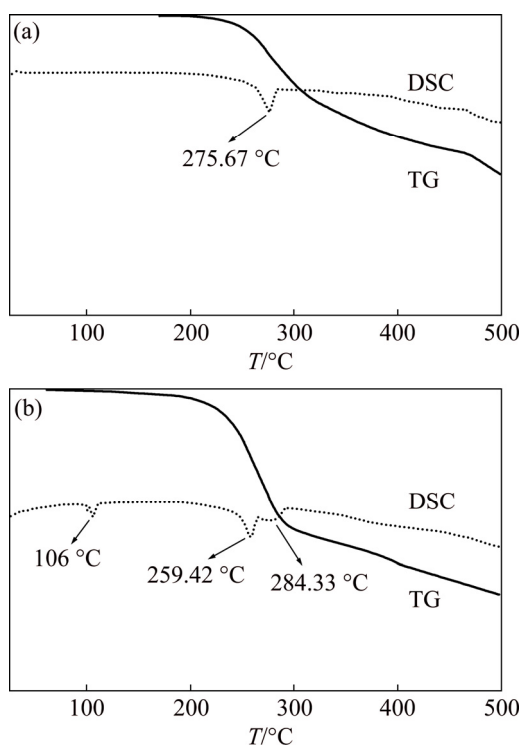
Fig. 8 Effect of roasting temperature on arsenic and antimony volatilization rates

Fig. 7 TG−DSC curves of samples: (a) Without sulfur; (b) Mixture of dust and sulfur (Sulfur addition content of 22%)

Fig. 9 X-ray diffraction patterns of roasted products at different temperatures (0% sulfur, 90 min)

As_2O_3 but higher than Sb_2O_3 [16]. Accordingly, Fig. 8 shows that when no sulfur is added, the arsenic volatilization rate decreases from 32.90% to 8.21% and antimony volatilization rate increases slightly from 5.04% to 5.84% with the increase of temperature from 250 to 350 °C. Figure 9 shows that the formation of amorphous substance starts at 300 °C and is almost completed at temperature above 350 °C. Increasing temperature further to 350 and 450 °C, vapor pressures of As_2O_3 and the formed amorphous substance increase [16], which causes volatilization rates of arsenic and antimony to increase. When 22% sulfur is added, it is clear that the trend of arsenic volatilization rate with roasting temperature is different deduced from Fig. 8. It increases with temperature from 250 to 350 °C. The reason might be that the Sb_2O_3 is vulcanized to Sb_2S_3, as shown in Fig. 10, and the amorphization reaction between As_2O_3 and Sb_2O_3 is prevented to some extent. This also causes the arsenic volatilization rate is higher than that without sulfur addition. Figure 10 shows that Sb_2S_3 can be found at 300 °C and its peak value increases from 300 to 350 °C. Meanwhile, peaks of the newly generated $AsSbO_3$ decrease with temperature from 300 to 350 °C, which may be related to the fact that the structure of $AsSbO_3$ is destroyed via a sulfidation reaction and transformed to As_2O_3 and Sb_2S_3. At approximately 400 °C, Sb_2S_3 and As_2S_3 could be generated at the same time (Eqs. (4) and (5)), and further
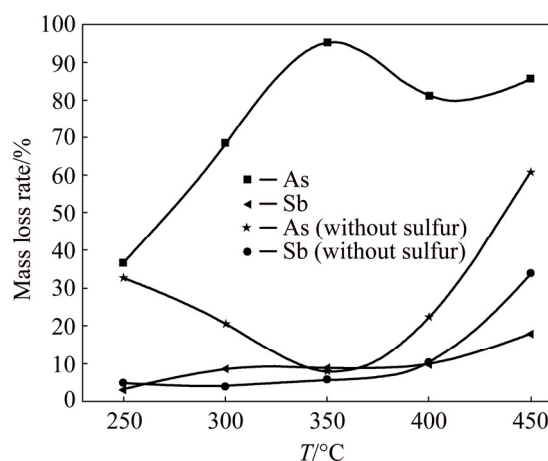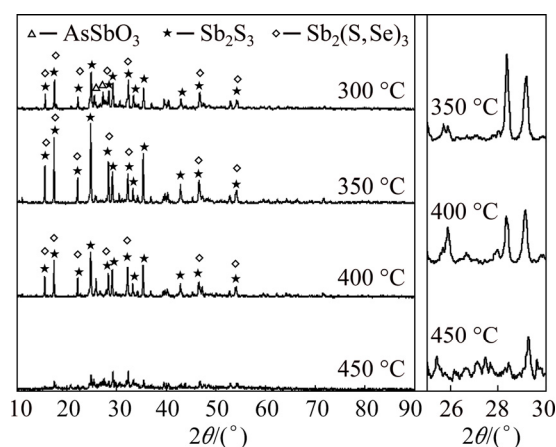

Fig. 10 X-ray diffraction patterns of roasted residues at different temperatures (22% sulfur, 90 min)

form an amorphous substance (As−Sb−S) [17] deduced from the amorphous peak appearing broad and high background in Fig. 10 and the SEM−EDS result in Fig. 11. It is difficult to volatile under the experimental

temperature [16], causing the arsenic volatilization rate to decrease. With the sulfur amount of 22%, the antimony volatilization rate increases slightly with temperature from 250 to 450 °C, seen from Fig. 8. For the purpose of increasing separation rate of arsenic and antimony, the roasting temperature should be performed at 350 °C.
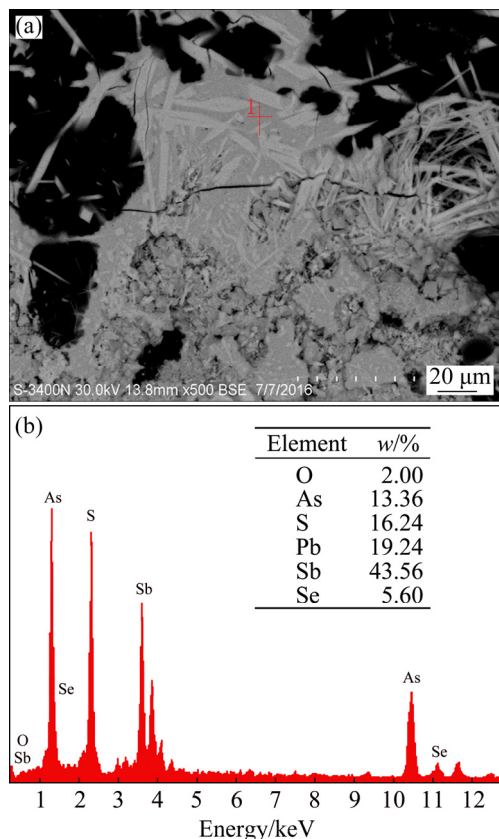

Fig. 11 SEM−EDS results of roasted residues (400 °C, 22% sulfur, 90 min)

3.3 Effect of sulfur content

The effect of sulfur content is studied at temperature of 350 °C, roasting time of 90 min and N_2 flow rate of 70 mL/min. The results in Fig. 12 show that the arsenic volatilization rate significantly depends on the sulfur content. With the increase of sulfur content from 14% to 22%, the amorphization reaction between As_2O_3 and Sb_2O_3 could be prevented deeper after more Sb_2O_3 has been sulfurized to Sb_2S_3 (Fig. 13), and this causes the arsenic volatilization rate to increase from 71.50% to 95.36%. Meanwhile, the antimony volatilization rate decreases from 12.93% to 9.07%. Increasing sulfur content further to 26% and 30%, As_2S_3 might be generated (Eq. (5)) and further react with Sb_2S_3 forming an amorphous substance (As−Sb−S) [17], as shown in Figs. 13 and 14, which decreases arsenic volatilization rate to 63.73% and 48.93%, respectively. Figure 13 shows that the peak value of Sb_2S_3 and $Sb_2(S,Se)_3$ increases with sulfur content from 14% to 22%, and then

decreases with sulfur content increasing. Meanwhile, the peak of $AsSbO_3$ decreases with sulfur content from 14% to 18% and disappears when sulfur content exceeds 22%. These could be attributed to the transformation of some Sb_2S_3 and $AsSbO_3$ to the amorphous substance (As−Sb−S) [17] as deduced from the increase of multiple split peaks and high background in Fig. 13 and SEM−EDS result in Fig. 14. Hence, the suitable sulfur content is 22%.
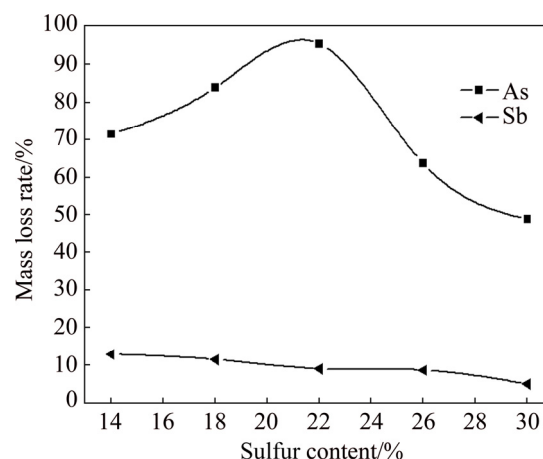

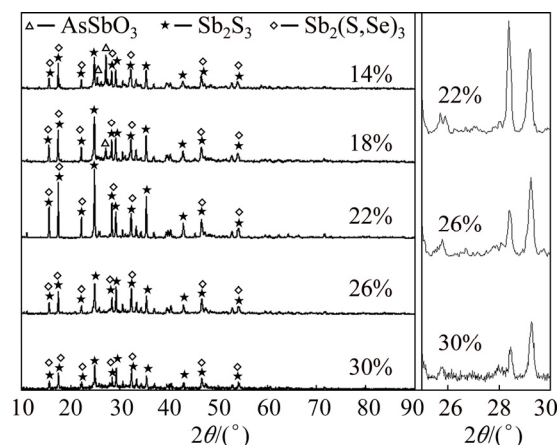**Fig. 12** Effect of sulfur content on arsenic and antimony volatilization rates

Fig. 13 X-ray diffraction patterns of roasted residues with different contents of sulfur (350 °C, 90 min)

3.4 Effect of roasting time

The effect of roasting time on volatilization rates of arsenic and antimony was investigated at 350 °C, sulfur content of 22%, and N_2 flow rate of 70 mL/min. The roasting time is varied from 60 to 120 min with interval of 15 min. The experiment results are presented in Fig. 15. It is obvious that the increase of roasting time results in increased volatilization rates for both arsenic and antimony. Precisely, the arsenic volatilization rate increases rapidly in the primary 90 min, and then remains nearly constant. Comparatively, that for antimony increases slightly from 8.30% to 14.87%. For

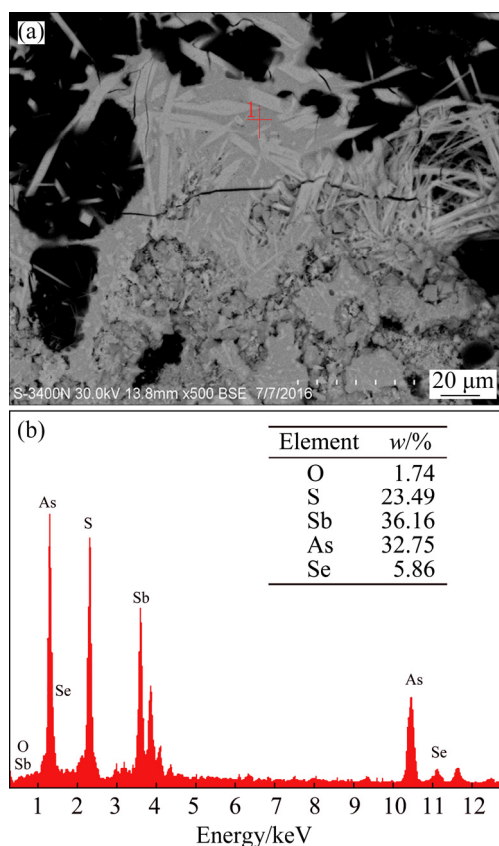the purpose of increasing separation efficiency of arsenic and antimony, the roasting time is fixed at 90 min.

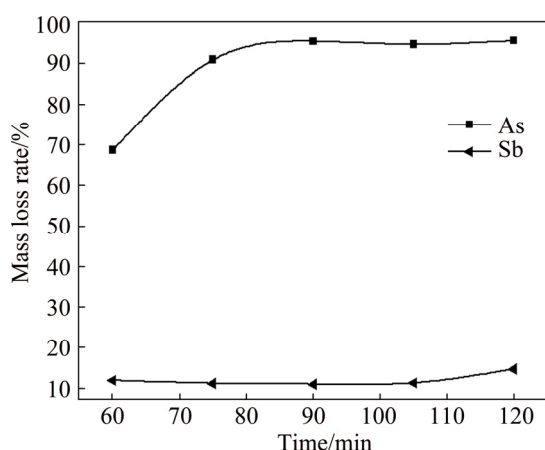**Fig. 14** SEM−EDS results of roasted residues (350 °C, 26% sulfur, 90 min)

Fig. 15 Effect of roasting time on arsenic and antimony volatilization rates

3.5 Effect of nitrogen flow rate

The effect of N₂ flow rate was investigated by keeping roasting temperature at 350 °C, sulfur content at 22% and roasting time at 90 min. Figure 16 shows that the N₂ flow rate has little effect on volatilizations of arsenic and antimony. This finding means that the external mass transfer does not play a significant role in

vaporization of the dust [18]. Thus, 70 mL/min of nitrogen is used as the standard flow rate in all experiments.
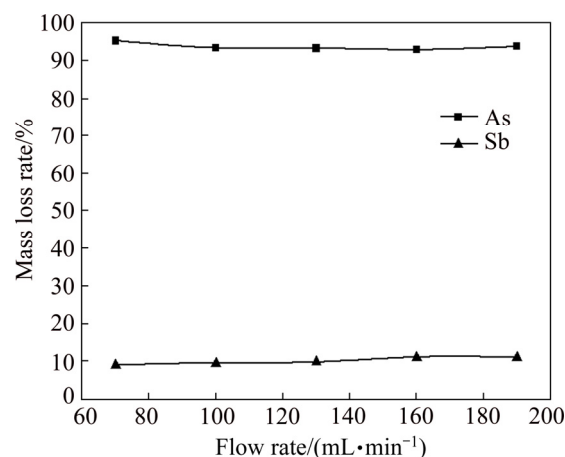

Fig. 16 Effect of N₂ flow rate on arsenic and antimony volatilization rates

Based on the experimental results given above, the arsenic in the dust with high content of arsenic and antimony can be effectively separated by a selective sulfidation roasting process using sulfur. The volatilization rates of arsenic and antimony are 95.36% and only 9.07% under the optimum condition of roasting temperature of 350 °C, sulfur content of 22%, roasting time of 90 min, and N₂ flow rate of 70 mL/min. Figures 17 and 18 show that the main phases of the volatiles and roasted residues are As₂O₃ and Sb₂S₃, respectively. The chemical composition of the roasted residue is given in Table 2.

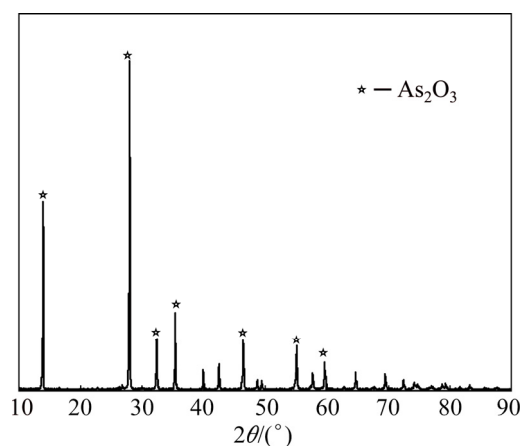**Fig. 17** X-ray diffraction pattern of volatile

This method possesses high volatilization rate of arsenic, low loss rate of antimony, and simple technological process compared with that in previous pyrometallurgical or hydrometallurgical processes. In addition, the antimony in the roasted residues could be reclaimed through a reverberatory process, and the volatiles can be used for producing Na₃AsO₄ [19].
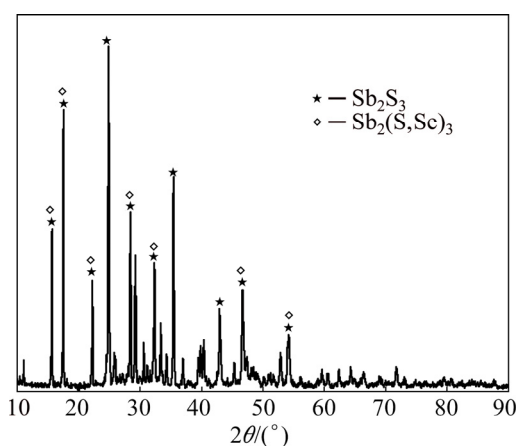
Fig. 18 X-ray diffraction pattern of roasted residue (350 °C, 22% sulfur, 90 min)

Table 2 Primary chemical composition of roasted residue (mass fraction, %)

Sb	S	As	Se	O	Pb	Others
57.91	15.64	5.57	5.11	4.02	3.52	8.23

4 Implications for industrial practice

In an industrial process, burner is used to provide heat, and the existence of O_2 is inevitable in the corresponding industrial process [20]. The phase stability (predominance) diagram for the As−Sb−S−O system constructed by HSC 7.0 at 350 °C is shown in Fig. 19. The shaded area of Fig. 19 is in the range of $p(O_2) \approx 10^{-22}-10^{-15}$ Pa and $p(S_8) \approx 10^{-30}-1$ Pa, in which the possible equilibrium pure phases are As_2O_3 and Sb_2S_3. It exhibits a suitable atmospheric condition for separating the arsenic from the dust.
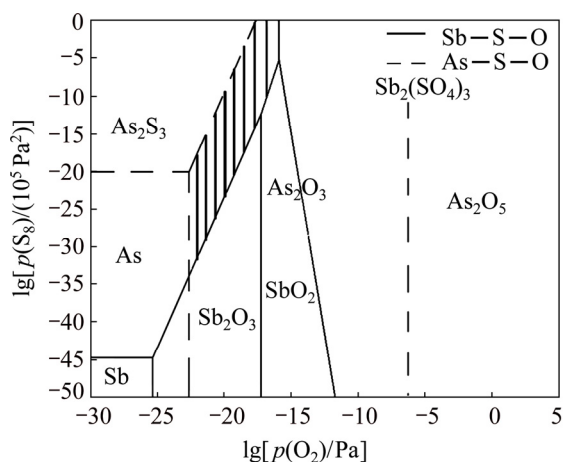

Fig. 19 Combined phase stability diagrams for As−Sb−S−O system at 350 °C

5 Conclusions

1) The volatilization rate of arsenic is about 95.36%

and that of antimony is only about 9.07% under the condition of roasting temperature of 350 °C, sulfur content of 22%, roasting time of 90 min and nitrogen flow rate of 70 mL/min.

2) With sulfur amount being less than 22%, the sulfur addition plays an active effect on the arsenic volatilization because the structure of solid solution ($(Sb,As)_2O_3$) in the dust could be destroyed after the Sb component in it being sulfurated to Sb_2S_3 and this generated As_2O_3 continues to volatile. In addition, the amorphization reaction between As_2O_3 and Sb_2O_3 also could be prevented to some extent after the Sb_2O_3 has been transformed to Sb_2S_3, which is beneficial to the arsenic volatilization.

3) The As_2S_3 might be generated and further react with Sb_2S_3 forming an amorphous substance (As−Sb−S) when the sulfur content exceeds 22% at roasting temperature over 350 °C, causing a decrease in arsenic volatilization rate.

References

[1]   MORILLO D, UHEIDA A, PÉREZ G, MUHAMMEDB M, VALIENTEA M. Arsenate removal with 3-mercaptopropanoic acid-coated superparamagnetic iron oxide nanoparticles [J]. Journal of Colloid & Interface Science, 2015, 438: 227−234.

[2]   WANG Yu, SIKORA S, KIM H, DUBEY B, TOWNSEND T. Mobilization of iron and arsenic from soil by construction and demolition debris landfill leachate [J]. Waste Management, 2012, 32: 925−932.

[3]   POUS N, CASENTINI B, ROSSETTI S, FAZIB S, PUIGA S, AULENTA F. Anaerobic arsenite oxidation with an electrode serving as the sole electron acceptor: A novel approach to the bioremediation of arsenic-polluted groundwater [J]. Journal of Hazardous Materials, 2015, 283: 617−622.

[4]   WANG Xiu, WANG Jian-ping, LIU Chong-hao, ZHANG Fang-fang. Situation analysis and sustainable development strategy of antimony resources in China [J]. China Mining Magazine, 2014, 23: 9−13. (in Chinese)

[5]   SAHU K K, AGRAWAL A, PANDEY B D. Recent trends and current practices for secondary processing of zinc and lead. Part II: Zinc recovery from secondary sources [J]. Waste Management & Research, 2004, 22: 248−254.

[6]   MIN Xiao-bo, LIAO Ying-ping, CHAI Li-yuan, YANG Zhi-hui, XIONG Shan, LIU Lin, LI Qing-zhu. Removal and stabilization of arsenic from anode slime by forming crystal scorodite [J]. Transactions of Nonferrous Metals Society of China, 2015, 25: 1298−1306.

[7]   MONTEGRO V, SANO H, FUJISAWA T. Recirculation of high arsenic content copper smelting dust to smelting and converting processes [J]. Minerals Engineering, 2010, 37: 29−33.

[8]   TIAN Heng-zhong, ZHAO Dan, CHENG Ke, LU Long, HE Meng-chang, HAO Ji-ming. Anthropogenic atmospheric emissions of antimony and its spatial distribution characteristics in China [J]. Environmental Science & Technology, 2012, 46: 3973−3980.

[9]   HU Hai-jin, QIU Ke-qiang. Three-step vacuum separation for treating arsenic sulphide residue [J]. Vacuum, 2015, 111: 170−175.

[10]   ETTLER V, MIHALJEVIC M, SEBEK O. Antimony and arsenic leaching from secondary lead smelter air-pollution-control residues [J]. Waste Management & Research, 2009, 28: 587−595.

[11] BROOKS G A, RANKIN W J. Solid-solution formation between arsenic and antimony oxides [J]. Metallurgical & Materials Transactions B, 1994, 25: 865−871.

[12] LI Lei, ZHANG Ren-jie, LIAO Bin, XIE Xiao-feng. Separation of As from As and Sb contained smoke dust by selective oxidation [J]. The Chinese Journal of Process Engineering, 2014, 14: 71−77. (in Chinese)

[13] GUO Xue-yi, YI Yu, SHI Jing, TIAN Qing-hua. Leaching behavior of metals from high-arsenic dust by NaOH−Na$_2$S alkaline leaching [J]. Transactions of Nonferrous Metals Society of China, 2016, 26: 575−580.

[14] ZHANG Xu, LIU Zhi-hong, LI Yu-hu, LIU Zhi-yong, LI Qi-hou. Oxygen pressure leaching of arsenic and antimony bearing flue dust in NaOH solution [J]. Journal of Central South University: Science and Technology, 2014, 45: 1390−1396. (in Chinese)

[15] BROOKS G A, RANKIN W J, GRAY N B. Thermal separation of arsenic and antimony oxides [J]. Metallurgical & Materials Transactions B, 1994, 25: 873−884.

[16] MAUSER J E. Heteronuclear compounds of arsenic and antimony [J]. Metallurgical & Materials Transactions B, 1982, 13: 511−513.

[17] ČERNOŠKOVÁ E, ČERNOŠEK Z, HOLUBOVÁ J. Thermoanalytical study and structure of stoichiometric As−Sb−S glasses [J]. Journal of Thermal Analysis & Calorimetry, 2014, 115: 285−288.

[18] ARACENA A, JEREZ O, ANTONUCCI C. Senarmontite volatilization kinetics in nitrogen atmosphere at roasting/melting temperatures [J]. Transactions of Nonferrous Metals Society of China, 2016, 26: 294−300.

[19] ZHOU Hong-hua. Research on synthetic recycle of dust being rich in Sb and As [J]. Hunan Nonferrous Mentals, 2005, 21: 21−23. (in Chinese)

[20] AHMAD S, RHAMDHANI M A, POWNCEBY M I, BRUCKARDB W J. Selective sulfidising roasting for the removal of chrome spinel impurities from weathered ilmenite ore [J]. International Journal of Mineral Processing, 2016, 146: 29−37.

选择性硫化法有效分离高砷锑烟尘中的砷和锑

谈 诚，李 磊，钟大鹏，王 华，李孔斋

昆明理工大学 冶金与能源工程学院，冶金节能减排教育部工程研究中心，
复杂有色金属资源清洁利用省部共建国家重点实验室，昆明 650093

摘 要：以硫磺为添加剂对高砷锑烟尘进行硫化焙烧，可实现物料中砷、锑的高效分离。借助 XRD、EPMA 和 SEM−EDS 等表征手段，对焙烧温度、焙烧时间、硫磺添加量和氮气流量对物料中砷、锑分离效率的影响进行研究。结果表明，在一定添加范围内，硫磺对高砷锑烟尘中砷的挥发脱除具有显著促进作用，原因是硫磺可将高砷锑烟尘中固熔体(Sb, As)$_2$O$_3$结构中的 Sb 组元硫化转变为 Sb$_2$S$_3$，使 As$_2$O$_3$组分得以解离释放，促进砷挥发率的提高；同时，高砷锑烟尘中 Sb$_2$O$_3$物相可硫化生成 Sb$_2$S$_3$，对 As$_2$O$_3$ 和 Sb$_2$O$_3$ 之间的非晶反应形成阻碍，亦有利于砷的挥发。在焙烧温度 350 °C、焙烧时间 90 min、硫磺添加量 22%和 N$_2$ 流量 70 mL/min 的试验条件下，砷挥发率可达 95.36%，锑挥发损失率仅 9.07%，实现砷锑烟尘中砷、锑的高效分离。

关键词：烟尘；砷；锑；硫磺；选择性硫化焙烧；分离

(Edited by Bing YANG)